

Article

Responses of Parameters for Electrical Impedance Spectroscopy and Pressure–Volume Curves to Drought Stress in *Pinus bungeana* Seedlings

Ai-Fang Wang ¹, Bao Di ¹, Tapani Repo ², Marja Roitto ³ and Gang Zhang ^{1,*}

¹ College of Horticulture, Hebei Agricultural University, 071001 Baoding, China; wangaifang82@126.com (A.W.); dibao666@126.com (B.D.)

² Natural Resources Institute Finland (Luke), Management and Production of Renewable Resources, P.O. Box 68, FI-80101 Joensuu, Finland; tapani.repo@luke.fi

³ Ruralia Institute and Helsinki Institute of Sustainability Science, University of Helsinki, Lonnrotinkatu 7, FI-50100 Mikkeli, Finland; marja.roitto@helsinki.fi

* Correspondence: zhanggang1210@126.com; Tel.: +86 13932237331

Received: 11 February 2020; Accepted: 19 March 2020; Published: 23 March 2020



Abstract: Background and Objectives: Drought occurs more frequently in Northern China with the advent of climate change, which might increase the mortality of tree seedlings after afforestation due to hydraulic failure. Therefore, investigating water relations helps us understand the drought tolerance of tree seedlings. Electrical impedance spectroscopy (EIS) is widely used to assess the responses of plant tissues to stress factors and may potentially reveal the water relations of cells. The aim of this study is to reveal the relationships between EIS and water related parameters, produced by pressure–volume (PV) curves in lacebark pine (*Pinus bungeana* Zucc.) seedlings reacting to drought stress. Materials and Methods: Four-year-old pot seedlings were divided into three parts (0, 5, and 10 days of drought) before planting, the treated seedlings were then replanted, and finally exposed to post-planting drought treatments with the following soil relative water contents: (i) adequate irrigation (75%–80%), (ii) light drought (55%–60%), (iii) moderate drought (35%–40%), and (iv), severe drought (15%–20%). During the post-planting growth phase, the EIS parameters of needles and shoots, and the parameters of PV curves, were measured coincidentally; thus, the correlations between them could be obtained. Results: The extracellular resistance (r_e) of needles and shoots were substantially reduced after four weeks of severe post-planting drought stress. Meanwhile, the osmotic potential at the turgor-loss point (ψ_{tlp}) and the saturation water osmotic potential (ψ_{sat}) of shoots decreased after drought stress, indicating an osmotic adjustment in acclimating to drought. The highest correlations were found between the intracellular resistance (r_i) of the shoots and ψ_{tlp} and ψ_{sat} . **Conclusions:** EIS parameters can be used as a measure of drought tolerance. The change in intracellular resistance is related to the osmotic potential of the cell and cell wall elasticity. Extracellular resistance is a parameter that shows cell membrane damage in response to drought stress in lacebark pine seedlings.

Keywords: cell wall elasticity; drought tolerance; extracellular resistance; intracellular resistance; osmotic adjustment

1. Introduction

Drought conditions in the past two decades occurred more frequently in most regions in Northern China [1]. This situation will continue with the climate change. Drought conditions increase the mortality of trees and may affect the forest carbon fixation and ecosystem services [2]. In addition to mature forests, large-scale afforestation has been done in China in order to promote land greening and to improve the ecological environment. Lacebark pine (*Pinus bungeana* Zucc.) is one of the main forest

and landscape tree species in Northern China and three to four year-old container seedlings are widely used for reforestation purposes. The seedlings may be easily exposed to drought soon after planting and to pre-planting drought during long-distance transportation and by delayed planting in stands, therefore increasing their mortality after afforestation as a result of hydraulic failure [3]. Investigating water status after drought stress may help us to understand the drought tolerance of tree seedlings.

Pressure–volume (PV) curves are one of the basic indices characterizing the plant–water status. It is, therefore, commonly used in plant ecophysiological studies [4,5]. Since the first application of the curves [6], this technique has been widely used to examine the elasticity of cell walls [7,8] and the relationship between plant performance and its internal water status [9–11].

During the process of tissues losing water, from being saturated to wilting, the water of cell vacuole is continuously released, and the cells shrink due to water loss. As the shrinkage level of the cell wall and cytoplasm is not the same, plasmolysis occurs when water losses reach a certain degree, and at that moment, the corresponding tissue potential is the initial plasmolysis osmotic potential at the turgor-loss point (ψ_{tlp}). The initial osmotic potential at the turgor-loss point (ψ_{tlp}) is indicative of the wilting point and the plant cannot absorb sufficient water below this point. Therefore, a lower ψ_{tlp} value indicates a stronger capacity to maintain turgor [12,13]. Likewise, a low value for the saturation–water osmotic potential (ψ_{sat}) indicates a high concentration of cell sap and a greater ability for plant cells to maintain maximum turgor. It is well known that high turgor is important in maintaining metabolic processes and growth [14]. A high ratio of bound-water content (V_b) to free-water content (V_p) suggests a more favorable water uptake and retention by a tree [15]. Cell wall elasticity is also considered to be an important physiological trait to depict the acclimation of plants to water stress [16]. A large value for the cell elastic modulus (ϵ) is related to rigid cell walls with less elasticity.

Electrical impedance spectroscopy (EIS) is related to the electrolyte balance in cells. In EIS, a plant sample is set in an electrical field with a small amplitude of the alternating current and resistance (real); the reactance (imaginary) part of the impedance is measured at different frequencies [17,18]. The selected equivalent circuit is decided according to the shape of the spectrum and the a priori information concerning the internal composition of the specimen. At low frequencies, the current passes through the apoplast, whereas the high frequency current may pass through the cell membranes. Then, the apoplast and symplast form a parallel circuitry, allowing for the symplastic resistance to be calculated [19]. If the cell membranes are damaged, e.g., by different stressors, then symplastic ions leak into the apoplastic space, leading to decreased extracellular resistance [20,21]. Intracellular resistance relates to the concentration of electrolytes and their mobilities in cells [19].

EIS has been widely used to reveal the responses of plant tissues to environmental stress, such as cold acclimation [22–24], freeze-thaw injury [20], heat [21], salt [25], elevated ozone [19], and flooding [26]. It has also been applied to evaluate growth of intact root system of herbaceous plants [27], tree roots [28,29] and the mycorrhiza colonization [30], as well as the frost damages of roots in small tree seedlings [31]. Recently, single-frequency impedance measurement was used to study plant response to alkaline stress [32]. Although the application of EIS in studying drought stress was not addressed before, the following studies showed that water content of organs was associated with the magnitude of EIS parameters. The moisture content had a strong effect on several EIS parameters in both viable and non-viable snap bean seeds—occurring in such a way that the increase in moisture content decreased the resistance parameters [33]. Similarly, the moisture content affected the EIS parameters in wood [34]. In white spruce (*Picea glauca*), the impedance of the stem was linearly related to the osmotic potential at full turgor during seasonal dormancy induction [35]. Considering the advantages of the EIS method, i.e., being fast and non-destructive, it will prove to be valuable in studies of plant–water relations.

In the present study, PV–curves and the EIS parameters of lacedark pine seedling needles and shoots were measured, coincidentally, after exposing the seedlings to drought stress. We hypothesize

that the water-related PV and EIS-parameters are correlated, and therefore, either could be exploited to characterize the degree of drought tolerance in lacebark pine seedlings.

2. Materials and Methods

2.1. Plant Materials and Drought Treatments

Four-year-old lacebark pine seedlings (stem diameter 0.48 ± 0.1 cm and height 21.0 ± 3.2 cm) (mean \pm SE), originating from Shanxi Province ($37^{\circ}05' N$, $111^{\circ}45' E$), were cultivated in the Beijing Ming Tombs Nursery ($40^{\circ}13' N$, $116^{\circ}13' E$, 400 m above sea level). In early spring, a total of 1000 dormant bare-root seedlings were excavated from the nursery bed, dipped in mud, and transported in plastic bags to the Garden of the Hebei Agricultural University ($38^{\circ}50' N$, $115^{\circ}26' E$, 22 m a. s. l.). The seedlings were immediately planted in mineral soil consisting of a mix of garden soil (top 20 cm) and fine sand (2:1) in soft and black plastic nutrition pots (volume 4.6 L, diameter \times height: 18 cm \times 18 cm).

The total nitrogen content of the soil was 360 mg kg^{-1} , the rapidly available phosphorus content was 12.1 mg kg^{-1} , the rapidly available potassium content was 128 mg kg^{-1} , and the organic matter content was 15.12 g kg^{-1} . The seedlings were placed in a plastic shed and were watered twice a week. The field moisture capacity of the soil in the pots was 22.6%, and the soil bulk density was 1.24 g cm^{-3} . Soil relative water content (SRWC) was used to indicate water deficiency during drought stress. SRWC was calculated according to the measured volumetric soil water content (TDR100, Spectrum Technologies, Inc., Plainfield, USA) as:

$$\text{SRWC} = [(\text{soil volumetric water content}/\text{soil bulk density})/22.6] \times 100 \quad (1)$$

The seedlings were watered every day to keep SRWC at the target level.

In the early growth phase, in the beginning of May, the seedlings were divided into three groups for drought stress treatments: (i) adequate irrigation (SRWC 75%–80%) (B1); (ii) light drought (SRWC 55%–60%) (B2), which was reached in 5 days of drought, and (iii) moderate drought (SRWC 35%–40%) (B3), which was reached in 10 days of drought. These were called the pre-planting drought treatments and they finished after B3 reached an SRWC level of 35%–40%.

At the end of the pre-planting drought treatments, 720 of the seedlings (240 seedlings of each pre-planting treatment) were transplanted in plastic buckets with a small drainage hole at the bottom (volume 12.3 L, diameter \times height: 25 cm \times 25 cm)—one plant was transported per bucket. Then, the seedlings of each pre-planting treatment were divided in four post-planting drought treatments in a split-plot design, with 60 seedlings in each treatment with the following SRWC: (i) adequate irrigation (75%–80%) (A1), (ii) light drought (55%–60%) (A2), (iii) moderate drought (35%–40%) (A3), and (iv) severe drought (15%–20%) (A4).

Once in the plastic shed, all the seedlings were divided into four replicate blocks. There were four plots for each post-planting treatment in each block. Each plot, with post-planting treatments (i.e., A1, A2, A3, and A4), was divided into three subplots, where the seedlings with pre-planting treatments (B1, B2, and B3) were placed randomly. Altogether, 12 treatment combinations were formed, i.e., A1B1, A1B2, A1B3, A2B1, A2B2, A2B3, A3B1, A3B2, A3B3, A4B1, A4B2, and A4B3. There were 15 seedlings in each of the four replicates of the treatments, i.e., a total of 60 seedlings in each treatment. The post-planting drought treatments were applied for 5 weeks after transplanting.

2.2. Electrical Impedance Spectroscopy

During the post-planting stress period, starting two weeks after transplanting, the EIS of needles and shoots were measured five times at one-week intervals. Eight seedlings per treatment (two seedlings of each replicate block) were randomly sampled at each harvest time and taken to the lab. Two current-year needles were sampled for each seedling, and a 15 mm-long sample was cut from the middle of the needle for EIS measurement at a constant temperature. In addition, two 15 mm-long shoot portions were cut from the middle of the current-year shoot of each sample seedling for EIS.

The sample was set between two Ag/AgCl electrodes (RC1; WPI Ltd., Sarasota, FL, USA) connected to an impedance analyzer (HP4284A LCR meter; Agilent, Palo Alto, CA, USA). Electrode gel (Sigma gel, Parker Laboratories, Inc. Fairfield, New Jersey, USA) was set between the cut surface of the sample and the electrode to minimize polarization impedance [20,36]. The real and imaginary part of the impedance was measured at 42 frequencies between 80 Hz and 1 MHz. Needle thicknesses and shoot diameters were measured using a thickness gauge (Mitutoyo NO. 7331, Kawasaki, Kanagawa, Japan).

According to the impedance spectra, an equivalent circuit model was determined for the samples. Model-A (Equation (2)) was used for the needles [24,37]:

$$Z_{\text{model-A}} = R_{\infty} + [(R_0 - R_{\infty}) \times (1 + \beta)] / [1 + \beta \times (1 + j \times \omega \times \tau_m)^{0.5}] \quad (2)$$

where R_{∞} (Ω) is the resistance at high frequencies, R_0 (Ω) is the resistance at low frequencies, the coefficient β is a factor controlling the skewness of the spectrum and the impedance locus center depression, and τ_m (s) is a time constant for the cell membrane. Here, the extracellular resistance (R_e) corresponded to R_0 , whereas intracellular resistance R_i was calculated as $R_{\infty} \times R_0 / (R_0 - R_{\infty})$. Specific resistances were calculated as:

$$r_x = A_{\text{needle}} \times R_x / l \quad (3)$$

where r_x refers to r_{∞} , r_e , and r_i (Ωm). As the needle cross-section is fan-shaped, with a 60° central angle, we calculated the needle area as $A_{\text{needle}} = \pi d^2 / 3$, where d is the needle thickness and l is the length.

According to the feature of impedance spectrum, two arcs in shoots, and the centers of the circles of the arcs are below the x-axes, distributed circuit element which is composed with two distributed elements in series with a resistor (double-DCE model) (Equation (4)) was applied for the shoots [20]:

$$Z = R + R_1 / [1 + (I \times \tau_1 \times \omega)^{\psi_1}] + R_2 / [1 + (I \times \tau_2 \times \omega)^{\psi_2}] \quad (4)$$

The model included three resistances (R , R_1 , and R_2 , unit Ω), two relaxation times (τ_1 and τ_2 , unit μs) and two distribution coefficients (ψ_1 and ψ_2) of the relaxation times. The parameters R , R_1 , and R_2 indicate the intersections of the arcs with the x-axis [17,22]. The relaxation times τ_1 and τ_2 indicate the apices of the circles, and the parameters ψ_1 and ψ_2 define the depression of the circle centers below the x-axis. Extracellular and intracellular resistance was calculated as $R_e = R + R_1 + R_2$ and $R_i = R \times (1 + R / (R_1 + R_2))$, respectively. The corresponding specific resistances (Ωm) were calculated, as in Equation (3), with the cross-sectional area calculated as $A_{\text{shoot}} = \pi \times d^2 / 4$ where d is the shoot diameter [22,23].

The parameters of the Model-A (Equation (2)) and double-DCE (Equation (4)) were estimated by the complex nonlinear least squares (CNLS) curve fitting of LEVM v 8.06 (obtained from J. R. Macdonald, Department of Physics and Astronomy, University of North Carolina, Chapel Hill, NC, USA).

2.3. Pressure-Volume (PV) Curves and Their Parameters

One seedling from each of the 12 post-planting treatments was sampled for PV-curves (i.e., a total of 12 curves) in the fourth week of the post-planting stress. As PV curves show high repeatability [38], no replicate measurement was made for the same seedling and treatment. The PV-curves were measured at room temperature (22°C), according to the gradual boosting method [9]. Shoots with a relatively uniform top were cut and inserted into a bottle filled with water for 20 h in darkness. The fresh weights (W_{Total}) of shoots in full saturation were measured. Then, the shoots were placed in a pressure chamber, with 5 mm of the cut end of the shoot protruding out of the pressure chamber through a rubber seal. For sap collection, a 50 mm-long latex tube, filled with absorbent paper, was weighed (W_1) and placed against the cut end of the shoot sample. After the lid was tightly secured, the chamber pressure was increased by 0.2 MPa for 10–15 minutes in order to collect the water exuded from the shoot. Then, the pressure was slightly reduced (0.05–0.1 MPa) and the latex collection tube was removed and weighed (W_2). The exuded water was calculated as W_2 / W_1 and was transformed to volume (V), and the corresponding applied pressure (P) was recorded. This procedure was repeated

until a total of 10–16 PV-pairs were obtained. After the measurement, the shoot was dried at 85 °C and the dry weight was (W_{Dry}) measured. The fresh weight of the shoot at each applied pressure (W_{Fresh}) was calculated as $W_{\text{Total}} - W_2$. The relative water content (RWC) of the shoot at each pressure level was calculated as: $\text{RWC}(\%) = (W_{\text{Fresh}} - W_{\text{Dry}}) / (W_{\text{Total}} - W_{\text{Dry}}) \times 100$. The PV-curve was graphed with the accumulated expressed sap ($1 - \text{RWC}$) on the x -axis and the $1/\text{applied pressure}$ (P) on y -axis (Figure 1).

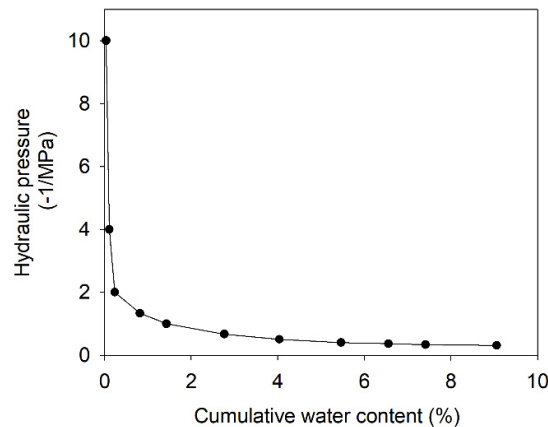


Figure 1. An example pressure–volume (P–V) curve of shoots in lacebark pine seedlings.

Depending on the applied pressure, each PV-curve had two distinct ranges: a nonlinear and a linear range [39]. The osmotic potential at the turgor-loss point (ψ_{tlp} , MPa) for initial plasmolysis was the turning point where the curve changed to a straight line. The corresponding accumulated expressed sap at the turning point was V_{tlp} . The relative water content of the initial plasmolysis was ($\text{RWC}_{\text{tlp}}, \%$) = $1 - V_{\text{tlp}}$. The intersection point of the extension line of the PV curve straight line and the Y -axis was the saturation water osmotic potential (ψ_{sat} , MPa). The symplastic water content at full turgor ($V_s, \%$) was obtained from the intersection of the extrapolated line of the PV curve straight line and the x -axis. The apoplastic water content was ($V_a, \%$) = $1 - V_s$. The free water was ($V_p, \%$) = $V_s - V_{\text{tlp}}$ [9,40]—the ratio of V_a and V_p was calculated accordingly. The cell elastic modulus was (ϵ , unit MPa) = $\Delta\psi_p / \Delta\text{RWC}$. When the water was extruded from plant tissue, ϵ changed continuously. Therefore, the maximum tissue bulk modulus of elasticity (ϵ_{max}) was usually used to compare the elastic properties, and was calculated as: $\epsilon_{\text{max}} = (\psi_{\text{sat}} - \psi_{\text{tlp}}) \times (V_s - V_{\text{tlp}}) / V_s$.

2.4. Statistical Analyses

A mixed linear model (procedure MIXED in SPSS 15.0.1, SPSS Inc., Chicago, IL, USA) analyzed the effects of the treatments on the EIS parameters. The model used was $y = \mu + A_i + B_j + \text{time}_k + A_i \times \text{time}_k + B_j \times \text{time}_k + A_i \times B_j + A_i \times B_j \times \text{time}_k + \epsilon_{ijk}$, where μ is a constant. In the model, ‘ A_i ’ represents the drought treatment effect during the post-planting period; $i = 1, 2, 3, 4$; ‘ B_j ’ is the drought treatment effect during the pre-planting period; $j = 1, 2, 3$; time_k is the time effect; and $k = 1, 2, 3, 4, 5$, and ϵ_{ijk} refers to the residual term. The factors ‘ A ’, ‘ B ’, and ‘time’ were regarded as a fixed term and ϵ a random term. The significance of the difference between the treatments at different sampling times was tested by contrasts using Bonferroni-corrected significance levels. The normality and homogeneity of the variance of the residuals were checked. The selection of the covariance structure was based on Akaike’s information criteria. Response variables were log transformed to fulfill the assumption of homogeneity in the analyses. The mean value of the seedlings in one block was used in the statistical analyses of the variables. There were four replicate blocks.

Correlation analyses between the PV curve parameters and EIS parameters were conducted based on Pearson’s correlation coefficients. All the data for correlation analysis were taken in the fourth week of the post-planting period.

3. Results

3.1. Electrical Impedance Spectroscopy (EIS) Parameters

Post-planting drought treatments (A1, A2, A3, and A4), pre-planting drought treatments (B1, B2, and B3), and their interactions ($A \times B$), had significant effects on the specific extracellular resistance (r_e) of stems during the post-planting growing period (Table 1). Pre-planting drought treatments (A1B2, A1B3) caused the reduction in the r_e of stems, as compared to the A1B1 treatment ($p < 0.05$ for each) after four weeks of post-planting growth. The r_e of the stems was significantly lower in the post-planting drought treatments (A2B1, A3B1, and A4B1), as compared to A1B1 seedlings four weeks after the post-planting growth ($p < 0.05$, $p < 0.001$, and $p < 0.001$, respectively). In the seedlings that went through pre-planting drought stress (B2), the r_e of the stems was almost significantly lower in A4B2 at week four ($p = 0.057$); however, A2B2 and A3B2 was not lower than A1B2. Additionally, in seedlings that went through pre-planting drought stress (B3), the r_e of the stems was higher in A2B3 and A4B3 than in A1B3, and was higher than in A2B1, A4B1 seedlings, but was still lower than in A1B1 (Figure 2a).

Table 1. The statistical significance of the effects of A, B, sampling time, and their interactions on electrical impedance spectroscopy (EIS) parameters during the post-planting growth period, where A is the effect of post-planting drought treatments, B is the effect of pre-planting drought treatments, and t is sampling time effect. p values ≤ 0.05 are in boldface. r_e : specific extracellular resistance; r_i : specific intracellular resistance; τ_1 and τ_2 : relaxation times; ψ_1 and ψ_2 : two distribution coefficients of the relaxation times; τ_m : a time constant for the cell membrane; β : a factor controlling the skewness of the spectrum and the impedance locus center depression.

| Response | Data | p Values | | | | | | |
|----------|--------|--------------|--------------|--------------|--------------|--------------|--------------|-----------------------|
| | | t | A | B | $A \times B$ | $t \times A$ | $t \times B$ | $t \times A \times B$ |
| r_e | Stem | 0.000 | 0.000 | 0.000 | 0.009 | 0.000 | 0.000 | 0.000 |
| r_i | Stem | 0.000 | 0.661 | 0.436 | 0.002 | 0.000 | 0.000 | 0.000 |
| τ_1 | Stem | 0.310 | 0.640 | 0.660 | 0.012 | 0.000 | 0.020 | 0.000 |
| τ_2 | Stem | 0.000 | 0.340 | 0.008 | 0.835 | 0.000 | 0.011 | 0.000 |
| ψ_1 | Stem | 0.494 | 0.110 | 0.946 | 0.109 | 0.264 | 0.400 | 0.059 |
| ψ_2 | Stem | 0.000 | 0.110 | 0.111 | 0.003 | 0.004 | 0.004 | 0.000 |
| r_e | Needle | 0.000 | 0.000 | 0.227 | 0.001 | 0.000 | 0.136 | 0.000 |
| r_i | Needle | 0.000 | 0.000 | 0.080 | 0.010 | 0.000 | 0.000 | 0.000 |
| τ_m | Needle | 0.000 | 0.000 | 0.003 | 0.058 | 0.000 | 0.005 | 0.000 |
| β | Needle | 0.000 | 0.000 | 0.005 | 0.251 | 0.000 | 0.025 | 0.000 |

Post-planting drought treatments (A1, A2, A3, and A4) had significant effects on the r_e of needles, whereas pre-planting drought (B1, B2, and B3) had no effect—with no differences between A1B1, A1B2, and A1B3 being shown (Figure 2b). The interaction effects between post and pre-planting stress were significant (Table 1). The r_e of the needles was significantly lower in A3B1 and A4B1 than in A1B1 ($p < 0.05$, $p < 0.001$, respectively), in A2B2, A3B2, and A4B2 than in A1B2 ($p < 0.01$, $p < 0.001$, $p < 0.001$, respectively), and in A4B3 than in A1B3 at week four ($p < 0.001$) (Figure 2b).

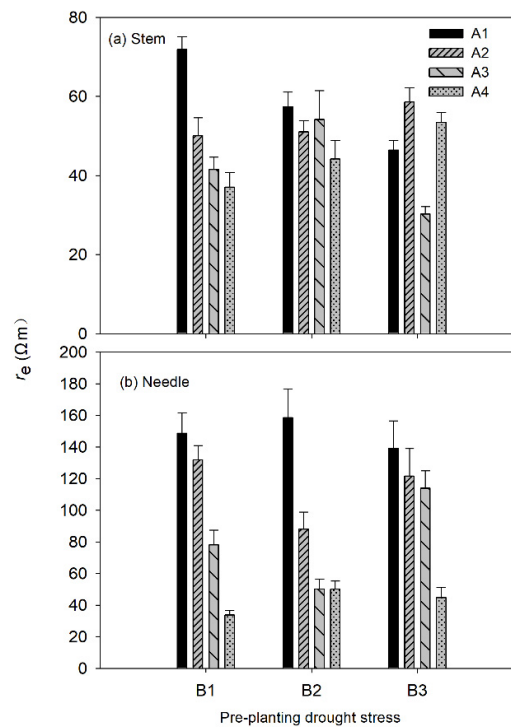


Figure 2. Extracellular resistance (r_e) of stems (a) and needles (b) in loblolly pine seedlings by four weeks of post-planting drought treatments (A1, A2, A3, and A4). A1, 75%–80% soil relative water content (SRWC); A2, 55%–60% SRWC; A3, 35%–40% SRWC; and A4, 15%–20% SRWC. B1, adequate irrigation before planting; B2, 5 days of drought before planting; and B3, 10 days of drought before planting.

Overall, either post-planting drought treatments (A1, A2, A3, and A4) or pre-planting drought treatments (B1, B2, and B3) had no significant effect on the r_i of the stems; however, the interaction effects between post and pre-planting stress were significant (Table 1). When comparing the pre-planting drought effects at week four, the r_i of the stems was higher in A3B2 than in A3B1 ($p < 0.05$), and higher in A4B2 and A4B3 than in A4B1 ($p < 0.05$, $p = 0.001$). When comparing post-planting drought effects, the r_i of the stems was higher in A4B3 than in A1B3, A2B3, and A3B3 ($p = 0.001$, $p < 0.05$, $p < 0.05$, respectively), and was slightly, but not significantly, higher in A3B2 and A4B2 than in A1B2 (Figure 3a).

Post-planting drought treatments (A) had significant effects on the r_i of the needles, whereas pre-planting drought (B) only had a slight effect on it. The interaction effects between post and pre-planting treatments were significant (Table 1). When comparing the pre-planting drought impact, the r_i of the needles was lower in A3B1 than in A3B3 ($p < 0.05$), and lower in A4B1 than in A4B3 ($p < 0.01$). When comparing the post-planting drought impact, the r_i of the needles was lower in A3B1 and A4B1 than in A1B1, and the statistically significant differences were found between the A4B1 and A1B1 treatments at week four ($p < 0.01$). In regard to the seedlings that went through pre-planting drought stress (B2), the r_i of the needles was lower in A2B2, A3B2, and A4B2 at week 4 ($p < 0.05$, $p = 0.08$, $p < 0.01$, respectively) than in the A1B2 treatment. There were no significant differences between post-planting drought treatments for the seedlings that went through pre-planting drought stress (B3) (Figure 3b).

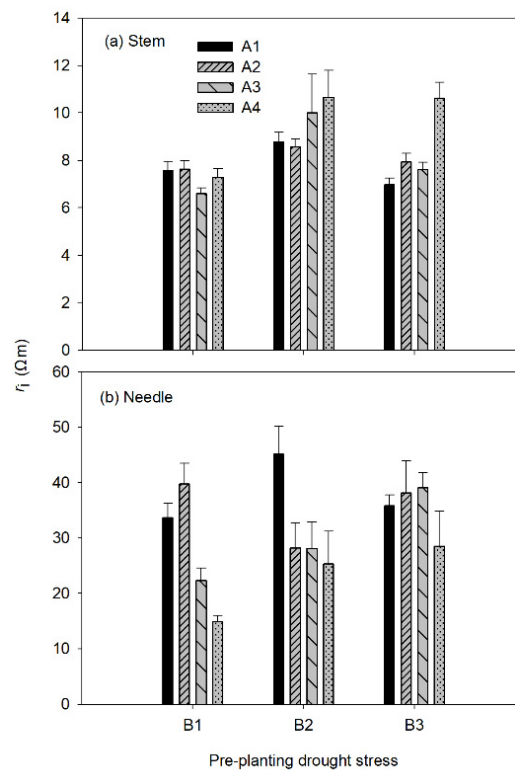


Figure 3. Intracellular resistance (r_i) of stems (a) and needles (b) in lacebark pine seedlings by four weeks of post-planting drought treatments (A1, A2, A3, and A4). A1, 75%–80% soil relative water content (SRWC); A2, 55%–60% SRWC; A3, 35%–40% SRWC; and A4, 15%–20% SRWC. B1, adequate irrigation before planting; B2, 5 days of drought before planting; and B3, 10 days of drought before planting.

3.2. Hydraulic Parameters of Shoots by PV Curves After Four Weeks Post-Planting Growth

Most of the shoots already underwent plasmolysis at a relative water content higher than 90%. The $RWC_{t_{lp}}$ of the shoots was the highest in A1B1 seedlings that were adequately irrigated throughout the experiment. Slight pre-planting drought (A1B2) decreased the value to 88% after four weeks of post-planting growth with adequate irrigation. Slight and moderate post-planting drought stresses (A2B1 and A3B1) decreased the $RWC_{t_{lp}}$ of the shoots. The $RWC_{t_{lp}}$ of the shoots was also lower in the seedlings that went through pre-planting drought and the further slight and moderate post-planting drought (A2B2, A3B2, A2B3, A3B3) than in A1B1 seedlings (Figure 4a).

Compared to A1B1 seedlings that were adequately irrigated throughout the experiment, the $\psi_{t_{lp}}$ of the shoots decreased, whether pre-planting drought stress (A1B2, A1B3) or the post-planting drought stress was applied (A2B1, A3B1, and A4B1). The $\psi_{t_{lp}}$ of the shoots also decreased in the seedlings that went through pre-planting drought (B2 and B3), and the further post-planting drought (A2B2, A3B2, A4B2, A2B3, A3B3, and A4B3) compared to A1B1. Notably, the seedlings without pre-planting drought stress (B1) had the lowest $\psi_{t_{lp}}$ of the shoots after four weeks of slight drought treatment (A2); however, the seedlings with pre-planting drought stress (B2 and B3) had the lowest value after four weeks of severe drought treatment (A4) (Figure 4b).

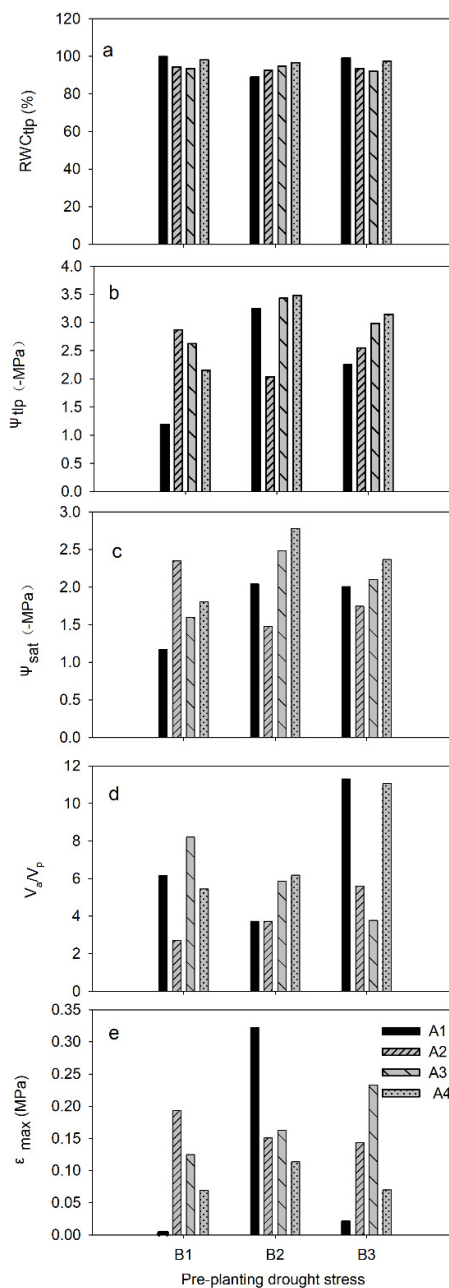


Figure 4. Relative water content at the turgor-loss point (RWC_{tlp}) (a), initial osmotic potential at the turgor-loss point (ψ_{tlp}) (b), saturation water osmotic potential (ψ_{sat}) (c), ratio of bound-water content to free-water content (V_a/V_p) (d), and the cell maximum bulk modulus of elasticity (ϵ_{max}) (e) of shoots in lacebark pine seedlings by four weeks of post-planting drought treatments (A1, A2, A3, and A4). A1, 75%–80% soil relative water content (SRWC); A2, 55%–60% SRWC; A3, 35%–40% SRWC; and A4, 15%–20% SRWC. B1, adequate irrigation before planting; B2, 5 days of drought before planting; and B3, 10 days of drought before planting.

Similar to the ψ_{tlp} of the shoots, the ψ_{sat} of the shoots decreased in pre-planting drought treatment (A1B2 and A1B3) and the post-planting drought treatments alone (A2B1, A3B1, and A4B1), as well as in the treatments with seedlings suffering from pre-planting drought treatments (B2, B3) and further post-planting drought treatments (A2B2, A3B2, A4B2, A2B3, A3B3, and A4B3)—as compared to the adequately irrigated seedling treatment (A1B1). The seedlings without pre-planting drought stress (B1) had the lowest ψ_{tlp} of the shoots after four weeks of slight drought stress (A2); however, the seedlings

with pre-planting drought stress (B2 and B3) had the lowest value after four weeks of severe drought stress (A4) (Figure 4c).

The ratio of bound-water content to free-water content (V_a/V_p) of the shoots was lower in the seedlings that suffered from slight pre-planting drought (A1B2), whereas it was higher in the seedlings that suffered from moderate pre-planting drought (A1B3) than in the A1B1 seedlings. The V_a/V_p of the shoots was higher in the seedlings that suffered from moderate post-planting drought (A3B1) and severe post-planting drought (A4B3) than in the A1B1 seedlings (Figure 4d).

The modulus of cell elasticity (ϵ_{\max}) markedly increased in the seedlings that went through slight pre-planting drought (A1B2), as compared to A1B1 seedlings. The post-planting drought (A2B1, A3B1, and A4B1) induced an increased ϵ_{\max} , with A2B1 increasing the most, and A4B1 increasing the least. The ϵ_{\max} was also higher in the seedlings that went through pre-planting drought treatment and further post-planting drought (A2B2, A3B2, A4B2, A2B3, A3B3, and A4B3) than in A1B1 seedlings. It is noted that ϵ_{\max} was lower in A2B2, A3B2, and A4B2 than in A1B2 seedlings (Figure 4e).

3.3. Correlation Analysis

Correlations among the EIS parameters and the PV-parameters are shown in Table 2. The r_i of the stems correlated negatively and significantly with ψ_{tlp} and ψ_{sat} in the shoots; however, the r_e of the stems showed slightly positive relationships with ψ_{tlp} and ψ_{sat} in the shoots. Moreover, the r_i of the stems showed a slightly positive relationship with ϵ_{\max} . The r_i and β of the needles correlated negatively with RWC_{tlp} in the shoots. The relaxation time (τ_1) of the stems had slightly positive correlations with the V_a/V_p of the shoots.

Table 2. Pearson correlation coefficients between the electrical impedance spectroscopy parameters and pressure–volume curves parameters at week 4 after the post-planting growing period. Asterisks indicate a significant correlation coefficient $p < 0.05$. Boldface indicates a significant correlation coefficient $0.05 < p < 0.1$. RWC_{tlp} : relative water content of the initial plasmolysis; ψ_{tlp} : osmotic potential at the turgor-loss point; ψ_{sat} : saturation water osmotic potential; V_a/V_p : ratio of bound-water content to free-water content; ϵ_{\max} : the maximum tissue bulk modulus of elasticity. r_e : specific extracellular resistance; r_i : specific intracellular resistance; τ_1 and τ_2 : relaxation times; ψ_1 and ψ_2 : two distribution coefficients of the relaxation times; τ_m : a time constant for the cell membrane; β : coefficient β controlling the skewness of the spectrum and the impedance locus center depression.

| | Stem | | | | | | Needle | | | |
|---------------------------|-------------|----------------|-------------|----------|----------|----------|--------|--------------|----------|----------------|
| | r_e | r_i | τ_1 | τ_2 | ψ_1 | ψ_2 | r_e | r_i | τ_m | β |
| RWC_{tlp} | 0.24 | −0.03 | −0.03 | 0.18 | 0.09 | −0.18 | 0.24 | −0.43 | −0.18 | −0.51 * |
| ψ_{tlp} | 0.46 | −0.56 * | −0.24 | −0.30 | 0.12 | −0.14 | 0.29 | −0.32 | 0.24 | −0.02 |
| ψ_{sat} | 0.43 | −0.58 * | −0.09 | −0.17 | 0.07 | −0.11 | 0.36 | −0.19 | 0.28 | 0.18 |
| V_a/V_p | 0.05 | 0.08 | 0.41 | 0.12 | −0.07 | −0.03 | −0.16 | −0.07 | −0.09 | −0.38 |
| ϵ_{\max} | −0.37 | 0.40 | 0.32 | 0.34 | −0.1 | 0.10 | −0.18 | 0.35 | −0.17 | 0.19 |

4. Discussion

Moderate and severe post-planting drought stresses (A3 and A4) for four weeks reduced the r_e of the shoots and needles, especially in the seedlings without pre-planting drought stress (B1). The decrease of r_e may be attributed to cellular membrane injuries, as previously observed in frost [20] and heat stress [21]. Cell dehydration by drought conditions caused the cytoplasm to shrink and break the molecular arrangement of the lipid layers on the membrane; thus, symplastic ions leach into the apoplasmic space, and r_e decreases. The injury of the cellular membrane was proven by the increased electrolyte leakage of the needles and stems from drought stress, as reported earlier [41,42]. Membrane stability index (MSI) of roots reflecting the electrolyte leakage also supported EIS results [32]. Due to its close relationship with the membrane injury by frost stress, r_e was often used to estimate semi-lethal

temperatures after freezing treatments, i.e., cold hardiness of conifer trees [43,44]. It seems that r_e is also a good parameter to estimate cell damage after drought stress.

The intracellular resistance of stems was increased in the A3 and A4 treatments in the seedlings that experienced pre-planting drought stress (B2 and B3). In the previous study on cold hardiness, the intracellular resistance of the stems of Scots pine increased during cold acclimation, which was suggested to be due to the restriction on the mobility of the ions [22]. Severe post-planting drought stress decreased the water content and increased the soluble sugar content of the stems in lacedbark pine seedlings [42], which might increase the cell sap concentration, and restrict the mobility of ions—thus increasing intracellular resistance [22,45]. Severe post-planting drought reduced the r_i in the needles of seedlings without pre-planting drought (B1). Similarly, increasing the NaCl concentration in the growth media reduced the r_i of leaves in olive trees (*Olea europaea* L.), which was suggested to be due to the alteration of membrane properties [25].

According to the correlation analysis, the r_e of the stems had slight positive correlations with the ψ_{tlp} and ψ_{sat} of the shoots. On the contrary, there were higher negative correlations between the r_i of the stems and the ψ_{tlp} and ψ_{sat} of the shoots. Previous studies showed that electrical resistance was related to the moisture content of the organ [33,34], and ψ_{sat} was linearly correlated with the impedance of the stem in white spruce, which accorded with our results [35]. Under moderate and severe post-planting drought conditions (A3 and A4), both ψ_{tlp} and ψ_{sat} were reduced, which accorded with the effects of drought on hemlock (*Tsuga heterophylla*) seedlings [46] and the *Eucalyptus globulus* clones [47]. This suggests that the stressed seedlings could enhance turgor maintenance by osmotic adjustment. Changes in minimum and maximum turgor pressure, and improved osmotic adjustment, are possibly associated with cell membrane properties and fluctuations in intracellular fluid compositions [25].

The intracellular resistance r_i of the stems also showed negative correlations with cell wall elasticity. ϵ_{max} was markedly higher in pre-planting drought treatment (A1B2) when compared to the pre-planting drought effect, and overall, was higher in the slight and moderate post-planting drought treatments (A2, A3) than in A4 and A1. The increase of ϵ_{max} (less cell wall elasticity) was consistent with previous studies on cell wall elasticity in drought stress [14]. On the contrary, the increment in cell wall elasticity (decrease of ϵ_{max}) was found in grapevine [48,49], olive tree [50], and common beans [16] in response to water stress. Both responses can be interpreted as evidence of the acclimation to drought conditions [51–53]. In this study, in the mild drought condition, cell wall elasticity was decreased more than what can contribute to turgor maintenance, allowing for the water potential of the cell to decrease faster when the water loss is the same, and therefore facilitating the water uptake from the soil [53]. The values of RWC_{tlp} decreased slightly after mild and moderate drought stress. A similar reduction of RWC_{tlp} was found in tomato leaves under infiltration irrigation (stimulus of drought), in which a higher resistance to water stress was suggested [54]. V_a/V_p rose under drought stress, indicating that the apoplastic water content increased. The correlation between the relaxation time τ_1 and V_a/V_p was obtained. This result accorded with the study on Scots pine shoots, where τ_1 had a high correlation with the dry matter content of the shoots during cold acclimation [22].

5. Conclusions

The seedlings were injured in cells by four weeks of severe drought stress; however, they also showed some potential acclimation by adjusting the osmotic potential of the cell and cell wall elasticity. Intracellular resistance could be thought of as an important parameter indicating the cell osmotic adjustment functioning; however, extracellular resistance is a parameter to show the cell membrane damage in response to drought stress in lacedbark pine seedlings.

Author Contributions: Designing the experiment, A.-F.W., G.Z.; Implementation of the experiment and data collection, A.-F.W., B.D.; Data analysis and interpretation, A.-F.W., G.Z.; Manuscript writing, A.-F.W., B.D., T.R., M.R., G.Z. All authors have read and agreed to the published version of the manuscript.

Funding: This work was funded by the Start-up Fund for Introduced Talents of Hebei Agricultural University (YJ201813) and the Fund for Introduced Returned Overseas Scholars of Hebei Province (C20190339).

Acknowledgments: We thank Jaakko Heinonen for his advice on the statistical analyses.

Conflicts of Interest: The authors declare no conflict of interest.

References

- Zhang, L.; Xiao, J.; Zhou, Y.; Zheng, Y.; Li, J.; Xiao, H. Drought events and their effects on vegetation productivity in China. *Ecosphere* **2016**, *7*, e01591. [[CrossRef](#)]
- Dickman, L.T.; McDowell, N.G.; Sevanto, S.; Pangle, R.E.; Pockman, W.T. Carbohydrate dynamics and mortality in a piñon-juniper woodland under three future precipitation scenarios. *Plant Cell Environ.* **2015**, *38*, 729–739. [[CrossRef](#)]
- McDowell, N.; Pockman, W.T.; Allen, C.D.; Breshears, D.D.; Cobb, N.; Kolb, T.; Plaut, J.; Sperry, J.; West, A.; Williams, D.G.; et al. Mechanisms of plant survival and mortality during drought: Why do some plants survive while others succumb to drought? *New Phytol.* **2008**, *178*, 719–739. [[CrossRef](#)]
- Harayama, H.; Ikeda, T.; Ishida, A.; Yamamoto, S.I. Seasonal variations in water relations in current-year leaves of evergreen trees with delayed greening. *Tree Physiol.* **2006**, *26*, 1025–1033. [[CrossRef](#)]
- Zolfaghar, S.; Villalobos-Vega, R.; Cleverly, J.; Eamus, D. Co-ordination among leaf water relations and xylem vulnerability to embolism of Eucalyptus trees growing along a depth-to-groundwater gradient. *Tree Physiol.* **2015**, *35*, 732–743. [[CrossRef](#)]
- Scholander, P.F.; Hammel, H.T.; Bradstreet, E.D.; Hemmingsen, E.A. Sap pressure in vascular plants. *Science* **1965**, *148*, 339–346. [[CrossRef](#)]
- Bowman, W.D.; Roberts, S.W. Seasonal changes in tissue elasticity in chaparral shrubs. *Plant Physiol.* **1985**, *65*, 233–236. [[CrossRef](#)]
- Pallardy, S.G. Transpiration and Plant Water Balance. In *Physiology of Woody Plants*, 3rd ed.; Elsevier: Amsterdam, The Netherlands, 2007; pp. 325–366.
- Tyree, M.T.; Hammel, H.T. The measurement of the turgor pressure and water relations of plants by the pressure-bomb technique. *J. Exp. Bot.* **1972**, *23*, 267–282. [[CrossRef](#)]
- Rascio, A.; Platani, C.; Di Fonzo, N.; Wittmer, G. Bound water in durum wheat under drought stress. *Plant Physiol.* **1992**, *98*, 908–912. [[CrossRef](#)]
- Arabzadeh, N.; Emadian, S.F. Effect of water (drought) stress on water relations of *Haloxylon Aphyllum* and *H. Persicum*. *Iran. J. Sci. Technol.* **2010**, *34*, 245–255.
- Bartlett, M.K.; Zhang, Y.; Kreidler, N.; Sun, S.; Ardy, R.C.; Cao, K.; Sack, L. Global analysis of plasticity in turgor loss point, a key drought tolerance trait. *Ecol. Lett.* **2014**, *17*, 1580–1590. [[CrossRef](#)]
- Banks, J.M.; Percival, G.C.; Rose, G. Variations in seasonal drought tolerance rankings. *Trees* **2019**, *33*, 1063–1072. [[CrossRef](#)]
- Turner, N.C.; Jones, M.M. Turgor Maintenance by Osmotic Adjustment: A Review and Evaluation. In *Adaptation of Plants to Water and High Temperature Stress*; Turner, N.C., Kramer, P.J., Eds.; John Wiley and Sons: New York, NY, USA, 1980; pp. 87–103.
- Di, X.Y.; Wang, M.B.; Chen, J.W.; Zhang, W.F. Study on water parameters with PV curves in eight poplar clones. *Acta Bot. Boreali Occident. Sin.* **2007**, *27*, 98–103, (In Chinese with English abstract).
- Martínez, J.P.; Silva, H.; Ledent, J.F.; Pinto, M. Effect of drought stress on the osmotic adjustment, cell wall elasticity and cell volume of six cultivars of common beans (*Phaseolus vulgaris* L.). *Eur. J. Agron.* **2007**, *26*, 30–38. [[CrossRef](#)]
- MacDonald, J.R. Emphasizing Solid Materials and Systems. In *Impedance Spectroscopy*; John Wiley & Sons Inc.: New York, NY, USA, 1987.
- Grimnes, S.; Martinsen, O.G. *Bioimpedance and Bioelectricity Basics*; Academic Press: San Diego, CA, USA, 2000; p. 359.
- Repo, T.; Oksanen, E.; Vapaavuori, E. Effects of elevated concentrations of ozone and carbon dioxide on the electrical impedance of leaves of silver birch (*Betula pendula*) clones. *Tree Physiol.* **2004**, *24*, 833–843. [[CrossRef](#)]
- Repo, T.; Zhang, M.I.N.; Ryyppö, A.; Vapaavuori, E.; Sutinen, S. Effects of freeze-thaw injury on parameters of distributed electrical circuits of stems and needles of Scots pine seedlings at different stages of acclimation. *J. Exp. Bot.* **1994**, *45*, 823–833. [[CrossRef](#)]

21. Zhang, M.I.N.; Willison, J.H.M.; Cox, M.A. Measurement of heat injury in plant tissue by using electrical impedance analysis. *Can. J. Bot.* **1993**, *71*, 1605–1611. [[CrossRef](#)]
22. Repo, T.; Zhang, G.; Ryyppö, A.; Rikala, R.; Vuorinen, M. The relation between growth cessation and frost hardening in Scots pines of different origins. *Trees* **2000**, *14*, 456–464. [[CrossRef](#)]
23. Repo, T.; Zhang, G.; Ryyppö, A.; Rikala, R. The electrical impedance spectroscopy of Scots pine (*Pinus sylvestris* L.) shoots in relation to cold acclimation. *J. Exp. Bot.* **2000**, *51*, 2095–2107. [[CrossRef](#)]
24. Zhang, G.; Ryyppö, A.; Repo, T. The electrical impedance spectroscopy of Scots pine needles during cold acclimation. *Physiol. Plant.* **2002**, *115*, 385–392. [[CrossRef](#)]
25. Mancuso, S.; Rinaldelli, E. Response of young mycorrhizal and non-mycorrhizal plants of olive tree (*Olea europaea* L.) to saline conditions. II. Dynamics of electrical impedance parameters of shoots and leaves. *Adv. Hortic. Sci.* **1996**, *10*, 135–145.
26. Wang, A.F.; Roitto, M.; Lehto, T.; Zwiazek, J.J.; Calvo-Polanco, M.; Repo, T. Waterlogging under simulated late-winter conditions had little impact on the physiology and growth of Norway spruce seedlings. *Ann. For. Sci.* **2013**, *70*, 781–790. [[CrossRef](#)]
27. Ozier-Lafontaine, H.; Bajazet, T. Analysis of root growth by impedance spectroscopy (EIS). *Plant Soil* **2005**, *277*, 299–313. [[CrossRef](#)]
28. Čermák, J.; Ulrich, R.; Staněk, Z.; Koller, J.; Aubrecht, L. Electrical measurement of tree root absorbing surfaces by the earth impedance method: 2. Verification based on allometric relationships and root severing experiments. *Tree Physiol.* **2006**, *26*, 1113–1121. [[CrossRef](#)]
29. Ellis, T.W.; Murray, W.; Paul, K.; Kavalieris, L.; Brophy, J.; Williams, C.; Maass, M. Electrical capacitance as a rapid and non-invasive indicator of root length. *Tree Physiol.* **2012**, *33*, 3–17. [[CrossRef](#)]
30. Repo, T.; Korhonen, A.; Laukkanen, M.; Lehto, T.; Silvennoinen, R. Detecting mycorrhizal colonisation in Scots pine roots using electrical impedance spectra. *Biosyst. Eng.* **2014**, *121*, 139–149. [[CrossRef](#)]
31. Repo, T.; Korhonen, A.; Lehto, T.; Silvennoinen, R. Assessment of frost damage in mycorrhizal and non-mycorrhizal roots of Scots pine seedlings using classification analysis of their electrical impedance spectra. *Trees* **2016**, *30*, 483–495. [[CrossRef](#)]
32. Cseresnyés, I.; Takács, T.; Sepovics, B.; Kovács, R.; Füzy, A.; Parádi, I.; Rajkai, K. Electrical characterization of the root system: A noninvasive approach to study plant stress responses. *Acta Physiol. Plant.* **2019**, *41*, 169. [[CrossRef](#)]
33. Repo, T.; Paine, D.H.; Taylor, A.G. Electrical impedance spectroscopy in relation to seed viability and moisture content in snap bean (*Phaseolus vulgaris* L.). *Seed Sci. Res.* **2002**, *12*, 17–29. [[CrossRef](#)]
34. Tiitta, M.; Repo, T.; Viitanen, H. Effect of soft rot and bacteria on electrical impedance of wood at low moisture content. *Mater. Org.* **1999**, *33*, 261–287.
35. Colombo, S.J.; Blumwald, E. Electrical impedance of white spruce shoots in relation to pressure-volume analysis and free sugar content. *Plant Cell Environ.* **1992**, *15*, 837–842. [[CrossRef](#)]
36. Repo, T. Influence of different electrodes and tissues on the impedance spectra of Scots pine shoots. *Electro Magn.* **1994**, *13*, 1–14. [[CrossRef](#)]
37. Zhang, M.I.N.; Repo, T.; Willison, J.H.M.; Sutinen, S. Electrical impedance analysis in plant tissues: On the biological meaning of Cole-Cole α in Scots pine needles. *Eur. Biophys. J.* **1995**, *24*, 99–106. [[CrossRef](#)]
38. Sun, Z.H.; Wang, Q.C. The drought resistance of four broad-leaved species in the north of China with PV technique. *Sci. Silv. Sin.* **2003**, *39*, 33–38, (In Chinese with English abstract).
39. Turner, N.C. Measurement of plant water status by the pressure chamber technique. *Irrig. Sci.* **1988**, *9*, 289–308. [[CrossRef](#)]
40. Inoue, Y.; Kenzo, T.; Tamai, S.; Yamamoto, F.; Yamanaka, N.; Ichie, T. Drought tolerance of three fabaceous seedlings grown under different soil water conditions in semi-arid land of South America. *J. Jpn. Soc. Reveg. Technol.* **2018**, *43*, 499–508. [[CrossRef](#)]
41. Wang, A.F.; Zhang, G. Effects of drought on electrical impedance spectroscopy parameters in stems of *Pinus bungeana* Zucc. seedlings. *Front. Agric. China* **2010**, *4*, 468–474. [[CrossRef](#)]
42. Wang, A.F.; Zhang, G.; Qie, Y.X.; Xiang, D.Y.; Di, B.; Chen, Z.P. Effects of drought on physiological characteristics of needles of *Pinus bungeana* Zucc. seedlings. *Plant Physiol. J.* **2012**, *48*, 189–196, (In Chinese with English abstract).

43. Wang, A.F.; Zhang, G.; Wei, S.C.; Cui, T.X. Relation between frost hardiness and parameters of electrical impedance spectroscopy in saplings of different development stage of *Pinus sylvestris* L. var. *mongolica* Litv. *Acta Ecol. Sin.* **2008**, *28*, 5741–5749, (In Chinese with English abstract).
44. Ryypö, A.; Repo, T.; Vapaavuori, E. Development of freezing tolerance in roots and shoots of scots pine seedlings at nonfreezing temperatures. *Can. J. For. Res.* **1998**, *28*, 557–565. [[CrossRef](#)]
45. Repo, T.; Hiekkala, P.; Hietala, T.; Tahvanainen, L. Intracellular resistance correlates with initial stage of frost hardening in willow (*Salix viminalis*). *Physiol. Plant.* **1997**, *101*, 627–634. [[CrossRef](#)]
46. Kandiko, R.A.; Timmins, R.; Worrall, J. Pressure-volume curves of shoots and roots of normal and drought conditioned western hemlock seedlings. *Can. J. For. Res.* **1980**, *10*, 10–16. [[CrossRef](#)]
47. Pita, P.; Pardos, J.A. Growth, leaf morphology, water use and tissue water relations of *Eucalyptus globulus* clones in response to water deficit. *Tree Physiol.* **2001**, *21*, 599–607. [[CrossRef](#)]
48. Patakas, A.; Noitsakis, B. Cell wall elasticity as a mechanism to maintain favorable water relations during leaf ontogeny in grapevines. *Am. J. Enol. Vitic.* **1997**, *48*, 352–356.
49. Patakas, A.; Nikolaou, N.; Zioziou, E.; Radoglou, K.; Noitsakis, B. The role of organic solute and ion accumulation in osmotic adjustment in drought-stressed grapevines. *Plant Sci.* **2002**, *163*, 361–367. [[CrossRef](#)]
50. Dichio, B.; Xiloyannis, C.; Angelopoulos, K.; Nuzzo, V.; Bufo, A.B.; Celano, G. Drought-induced variations of water relations parameters in *Olea europea*. *Plant Soil* **2003**, *257*, 381–389. [[CrossRef](#)]
51. Tyree, M.T.; Karamanos, A.J. Water Stress as an Ecological Factor. In *Plants and Their Atmospheric Environment*; Grace, J.B., Ford, E.D., Jarvis, P.G., Eds.; Blackwell Scientific Publications: Oxford, UK, 1981; pp. 237–261.
52. Niinemets, U. Global-scale climatic controls of leaf dry mass per area, density, and thickness in trees and shrubs. *Ecology* **2001**, *82*, 453–469. [[CrossRef](#)]
53. Lenz, T.I.; Wright, I.J.; Westoby, M. Interrelations among pressure–volume curve traits across species and water availability gradients. *Physiol. Plant* **2006**, *127*, 423–433. [[CrossRef](#)]
54. Xu, H.L.; Xu, Q.C.; Qin, F.F.; Tian, C.M.; Wang, R. Applications of xeropytophysiology in plant production—Tomato fruit yield and quality improved by restricted irrigations in soil-based greenhouses. *Acta Hort.* **2011**, 893. [[CrossRef](#)]



© 2020 by the authors. Licensee MDPI, Basel, Switzerland. This article is an open access article distributed under the terms and conditions of the Creative Commons Attribution (CC BY) license (<http://creativecommons.org/licenses/by/4.0/>).